

One-dimensional transport of electrons in Si/Si_{0.7}Ge_{0.3} heterostructures

M. Holzmann,^{a)} D. Többen, and G. Abstreiter
Walter Schottky Institut, Technische Universität München, D-85748 Garching, Germany

M. Wendel, H. Lorenz, and J. P. Kotthaus
Sektion Physik der Ludwig-Maximilians-Universität München, Geschwister-Scholl-Platz 1, D-80539 München, Germany

F. Schäffler
Daimler-Benz AG, Forschungsinstitut Ulm, Wilhelm-Runge-Strasse 11, D-89081 Ulm, Germany

(Received 22 August 1994; accepted for publication 13 December 1994)

Magnetotransport of high-mobility electrons in quasi-one-dimensional quantum wires in Si/Si_{0.7}Ge_{0.3} heterostructures is studied. Arrays of shallow and deep etched wires with a period of 480 nm are defined by laser holography and patterned by reactive ion etching. Typical features of transport in narrow electron channels, such as oscillations due to the depopulation of quasi-one-dimensional subbands and an anomalous resistance maximum at low magnetic fields are observed. The narrowest channels have an effective width of ≈ 70 nm and a sublevel spacing of 1 meV. © 1995 American Institute of Physics.

Quantum wires have been the subject of intensive studies for several years.¹⁻⁵ Magnetotransport phenomena, like the depopulation of one-dimensional subbands, the suppression of weak localization, and backscattering due to diffuse boundary scattering, give information about fundamental electronic properties.⁶ The observation of these effects has already been possible on different host materials,^{4,7,8} such as GaAs, InGaAs, and Si-MOSFETs, and normally requires a high-mobility two-dimensional electron gas (2DEG) and sophisticated fabrication methods. Recently, Si/SiGe heterostructures with electron mobilities above 100 000 cm²/V s have become available⁹⁻¹² and indeed classical size effects have been demonstrated in field-effect induced wires.¹³ Similarly, one should be able to observe one-dimensional transport phenomena in narrow electron channels if the fabrication process does not reduce the mobility too drastically, i.e., if the elastic mean free path still exceeds the wire width. In this letter, we present magnetotransport results on quasi-one-dimensional quantum wires realized in the Si/SiGe system.

Figure 1 presents a schematic cross section of the *n*-type modulation doped heterostructure. The layers were grown at Daimler-Benz by molecular beam epitaxy on Si(100). The layer thicknesses were determined by secondary ion mass spectroscopy and from transmission electron micrographs. For the etching process it is important to know that the 22 nm thick antimony doping layer lies 49 nm underneath the surface and is separated from the 2DEG by an 11 nm thick undoped spacer. At $T=370$ mK the 2DEG exhibits an electron mobility of $\mu=175$ 000 cm²/V s at a carrier density of $n_s=6.9 \times 10^{11}$ cm⁻², resulting in a Fermi energy $E_F=4.4$ meV and an elastic mean free path l_{mfp} of 1.7 μm .

On all specimens, photoresist stripes with period $a=480$ nm were fabricated by means of standard laser holography. The wire grating was transferred into the SiGe heterostructure by reactive ion etching (RIE) using CF₄ as the gas source. With a constant etch rate at a fixed gas flow and

power input, we achieved etch depths d between 50 and 92 nm by varying the etch time. The profile of the etched structure, i.e., the period and etch depths, were measured by atomic force microscopy (AFM). 150 μm wide mesas were defined by wet chemical etching into the Si channel, so that about 300 wires are contacted in parallel. For the samples with $d=50, 55,$ and 60 nm the wire length L is 300 μm in order to minimize the influence of the contact resistance, and for $d=85$ and 92 nm we utilize shorter wires between 20 and 150 μm length because of the high series resistance in deep etched wires. Nevertheless L exceeds the elastic mean free path of the 2DEG by more than one order of magnitude and therefore the geometrical conditions should allow electron transport in the quasiballistic regime where $W < l_{\text{mfp}} < L$ has to be satisfied.⁶ W is the effective wire width in contrast to the geometrical wire width.

All measurements were performed in a commercial ³He system at $T=360 \pm 10$ mK with standard lock in technique

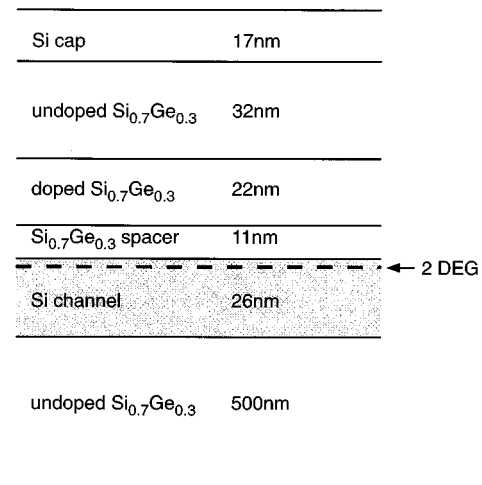


FIG. 1. Schematic cross section of the upper layers of the Si/Si_{0.7}Ge_{0.3} heterostructure. The two-dimensional electron gas is situated in the gray-shaded Si layer. The Si(100) substrate and the linearly graded buffer with a final Ge content of 30% are not shown.

^{a)}Electronic mail: holzmann@physik.tu-muenchen.de

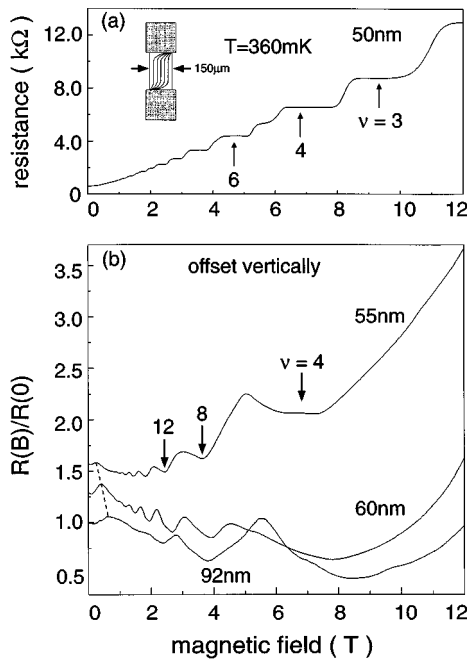


FIG. 2. (a) Two-terminal resistance of the specimen with 50 nm deep etch grooves. The inset shows schematically the sample geometry and equipotential lines in a magnetic field perpendicular to the 2DEG. (b) Magnetoresistance of samples with successively increased etch depth normalized to the value at $B=0$ T. The curves are vertically offset for clarity. The shift of the low-field magnetoresistance peak is marked by the dashed line. All measurements were performed at $T=360$ mK.

in two-terminal geometry [inset, Fig. 2(a)]. This low temperature was chosen because of the strong damping of the Shubnikov–de Haas oscillations at higher temperatures in silicon and to fulfill the condition $4 \text{ kT} < \hbar\omega_0$,⁶ with $\hbar\omega_0$ being the one-dimensional subband spacing at zero magnetic field.

The two-terminal resistance of samples with various etch depths is shown in Fig. 2. The specimen with 50 nm deep modulation [Fig. 2(a)] shows well-pronounced plateaus down to filling factor $\nu=36$. The position of these plateaus agrees well with $h/\nu e^2$ for magnetic fields above 2 T. Spin and valley degeneracies are lifted at higher magnetic fields. The shape of magnetotransport curves changes significantly if one etches deeper into the doped layer or into the 2DEG [Fig. 2(b)]. A low field maximum arises which shifts to higher magnetic fields with increasing d [dashed line in Fig. 2(b)]. For $d \geq 55$ nm the longitudinal resistivity ρ_{xx} becomes clearly dominant. Only the wires separated by 55 nm deep etch grooves show a rise in the resistance of successive minima above 2 T. Furthermore, the number of resolvable oscillations decreases strongly with increasing etch depth. For $d=92$ nm, where the etched grooves cut through the 2DEG, only four minima are identified up to 12 T.

The specimen with 50 nm deep etch grooves still shows two-dimensional transport characteristics. In two-terminal geometries both ρ_{xx} and ρ_{xy} contribute to the resistance. Above a certain magnetic field, the ρ_{xx} contribution, in the order of 100Ω for these samples, is negligibly small compared to ρ_{xy} . In this regime, one predominantly measures the voltage drop near the contact regions, and thus the resistance

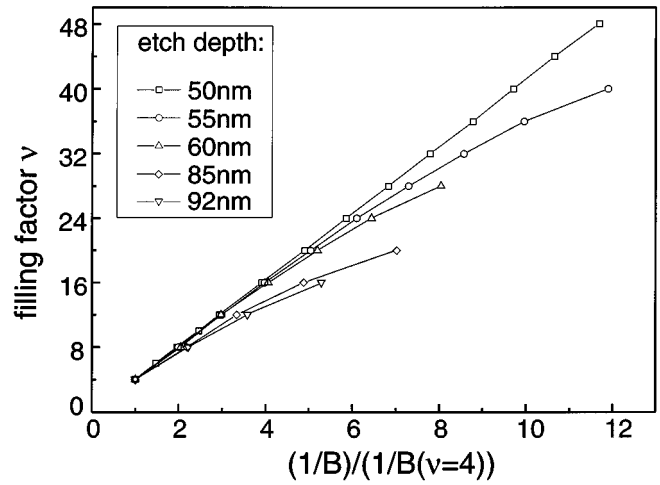


FIG. 3. Filling factors ν vs $(1/B)/[1/B(\nu=4)]$ for various etch depths. The symbols refer to the measured minima in magnetoresistance. The transition to quasi-one-dimensional transport for etch depths ≥ 55 nm gives rise to deviations from linear dependence.

is dominated by ρ_{xy} , yielding the plateaus. Etching deeper into the doped SiGe-layer results in the formation of quantum wires, indicated by the anomalous, low-field-resistance maximum which is due to diffuse scattering at the wire boundaries. The shift of this peak to higher magnetic fields for $d=60$ and 92 nm is a consequence of decreasing effective wire widths W_T according to $W_T = \sqrt{\pi n_s} / 2eB_{\text{Peak}}$ ¹⁴ provided that the sheet density remains nearly constant.

Figure 3 presents the Landau plots for successively deeper etched grooves. The clear deviations from linear behavior manifest the depopulation of quasi-one-dimensional subbands. The two-dimensional sheet density n_s for $d=50$ nm amounts to $7.0 \times 10^{11} \text{ cm}^{-2}$, which is almost equal to that of the unstructured 2DEG. Obviously, removing the cap layer and the upper undoped 32-nm-thick $\text{Si}_{0.7}\text{Ge}_{0.3}$ barrier [Fig. 1] does not affect the magnetotransport characteristics along the wires significantly. For $d \leq 55$ nm, the quasi-two-dimensional carrier concentration n_s can be determined using the linear part of the corresponding Landau plots. The carrier densities evaluated in this way all range between 7.0×10^{11} and $7.5 \times 10^{11} \text{ cm}^{-2}$, i.e., the RIE process used is apparently not accompanied by a reduction of the carrier density.

Assuming a parabolic confining potential, deviations from the linear behavior in Fig. 3 can be used to determine the one-dimensional subband spacing $\hbar\omega_0$, the carrier line density n_{1D} , and an effective wire width W_p .⁴ In tensile strained silicon, however, the valley degeneracy $g_v=2$ has to be taken into account. The results of parabolic fits to the Landau plots are summarized in Table I. The fits yield maximal sublevel spacings of about 1 meV and a carrier density of $9.0 \times 10^6 \text{ cm}^{-1}$.

We compare W_p to the effective wire width as determined from the position of the low field resistance peak W_T where n_s is the quasi-two-dimensional carrier concentration. The wire widths obtained from the low field maximum exhibit somewhat smaller values throughout the series of

TABLE I. Wire properties: Etch depth d , subband spacing, one-dimensional carrier density, wire width according to a parabolic fit, wire width deduced from the low field maximum, number of theoretically occupied subbands and number of experimentally observed quantum oscillations.

Etch depth (nm)	ω_0 (meV)	n_{1D} (10^6 cm^{-1})	Parabolic potential W_P (nm)	Low field maximum W_T (nm)	Occupied subbands: $N \cong W_P k_F / 4$	Observed oscillations
55	0.29	22.8	288	176	10.7	10
60	0.53	15.7	172	124	6.6	7
85	0.82	10.1	111	86	4.1	5
92	0.96	9.0	96	73	3.7	4

samples, with better agreement for the two specimens etched deepest. W_T is independent of the shape of the confining potential and consequently comparing W_P with W_T gives information about the validity of the model potential employed. A parabolic potential seems to be a reasonable approximation for wires with width ≤ 100 nm. Because of screening effects, the actual potential probably has a flat bottom which causes larger deviations for the shallower etched samples with $d=55$ and 60 nm.

For narrower wires, one also expects fewer one-dimensional subbands to be occupied and therefore less quantum oscillations. We estimate the number of theoretically occupied sublevels N in parabolic confining potential using $N \cong W_P k_F / 4$.⁶ This corresponds very well to the number of oscillations observed in the magnetotransport measurements (columns 6 and 7 in Table I). For wires with $W_T=73$ nm only four subbands are occupied at $B=0$ T.

Finally, we briefly discuss the depletion lengths l_{depl} and the mobility μ_W of the electron channels. AFM micrographs performed to measure the etch depth are also a suitable tool to determine the geometrical wire width W_{geo} . Depletion lengths in the plane of the 2DEG are estimated by $l_{\text{depl}} = (W_{\text{geo}} - W_T) / 2$. In this way one obtains l_{depl} of ≈ 30 nm and ≈ 80 nm for the 55 and 60 nm deep etch grooves, respectively. The deep etching process, i.e., etching through the 2DEG, results in a depletion length of ≈ 100 nm. These values are comparable to those known from GaAs nanostructures.¹⁵ The RIE process has not yet been studied in detail and we assume that a significant reduction of l_{depl} , which mainly depends on the Fermi level pinning at the surface, can be achieved by optimizing the fabrication parameters.

The mobility μ_W of the conducting electrons can easily be estimated in two ways. First, we use the measured resistance $R_0 = (L/W_T) M e n_s \mu_W$ at $B=0$ T, assuming that all $M=300$ wires are conducting. We consider only the $d=55$ nm specimen, for which the etch damage should be smallest. The measured resistance, however, contains the contact resistances R_C . To eliminate the influence of the Ohmic contacts, we determine an upper limit for R_C from the deviation of the $\nu=4$ plateau [Fig. 2(a)] from its exact value $h/4e^2$. From this we obtain $R_C=107 \text{ } \Omega$ and $\mu_W = 22\,700 \text{ cm}^2/\text{V s}$. Second, we use the condition for the observation of the subband depopulation $\Delta E \tau \approx \hbar$, where τ is the scattering time. The resulting mobility for a sublevel spacing of $\Delta E=0.29$ meV (Table I) is about $21\,000 \text{ cm}^2/\text{V s}$ in good agreement with the first estimate. The mo-

bility of the 2DEG is thus reduced by almost one order of magnitude as a consequence of the nanostructuring process.

In conclusion, we have observed quasi-one-dimensional transport in electron channels in Si/Si_{0.7}Ge_{0.3} heterostructures. By means of RIE, shallow and deep-etched quantum wires were fabricated. Subband spacing in the range of 0.3 to 1 meV with corresponding effective wire widths between 180 and 70 nm were achieved. In the smallest wires only four sublevels remain occupied.

The authors would like to thank W. Hansen for valuable discussions and S. Kühn for excellent technological support. Financial support by the Bundesministerium für Forschung und Technologie (Germany) under Grant No. NT 24137 and by the Siemens AG (SFE Mikrostrukturierte Bauelemente) is gratefully acknowledged.

¹H. Sakaki, Jpn. J. Appl. Phys. **19**, L735 (1980).

²K. K. Choi and D. C. Tsui and S. C. Palmateer, Phys. Rev. B **33**, 8216 (1986).

³W. Hansen, M. Horst, J. P. Kotthaus, U. Merkt, Ch. Sikorski, and K. Ploog, Phys. Rev. Lett. **58**, 2586 (1987).

⁴K.-F. Berggren, G. Roos, and H. van Houten, Phys. Rev. B **37**, 10118 (1988).

⁵T. J. Thornton, M. L. Roukes, A. Scherer, and B. P. Van de Gaag, Phys. Rev. Lett. **63**, 2128 (1989).

⁶C. W. J. Beenakker and H. van Houten, in *Solid State Physics*, edited by H. Ehrenreich and D. Turnbull (Academic, San Diego, CA, 1991), Vol. 44, p. 1.

⁷S. Block, M. Suhrke, S. Wilke, A. Menschig, H. Schweizer, and D. Grützmacher, Phys. Rev. B **47**, 6524 (1993).

⁸J. R. Gao, C. de Graaf, J. Caro, S. Radelaar, M. Offenberg, V. Lauer, J. Singleton, T. J. B. M. Janssen, and J. A. A. J. Perenboom, *Proceedings of the 20th International Conference on the Physics of Semiconductors*, edited by E. M. Anastassakis and J. D. Joannopoulos (World Scientific, Singapore, 1990), Vol. 3, p. 2339.

⁹Y. J. Mii, Y. H. Xie, E. A. Fitzgerald, D. Monroe, F. A. Thiel, B. E. Weir, and L. C. Feldman, Appl. Phys. Lett. **59**, 1611 (1991).

¹⁰F. Schäffler, D. Többen, H.-J. Herzog, G. Abstreiter, and B. Holländer, *Semicond. Sci. Technol.* **7**, 260 (1992).

¹¹Y. H. Xie, E. A. Fitzgerald, D. Monroe, P. J. Silverman, and G. P. Watson, J. Appl. Phys. **73**, 8364 (1993).

¹²S. F. Nelson, K. Ismail, T. N. Jackson, J. J. Nocera, J. O. Chu, and B. S. Meyerson, Appl. Phys. Lett. **63**, 794 (1993).

¹³M. Holzmann, D. Többen, G. Abstreiter, and F. Schäffler, J. Appl. Phys. **76**, 3917 (1994).

¹⁴H. Akera and T. Ando, Phys. Rev. B **43**, 11676 (1991).

¹⁵T. Demel, D. Heitmann, P. Grambow, and K. Ploog, Appl. Phys. Lett. **53**, 2176 (1988).